Selection of optimum frequency bands for detection of epileptiform patterns

Piyush Swami[1,2], Manvir Bhatia[3,4], Manjari Tripathi[5], Poodipedi Sarat Chandra[6], Bijaya K. Panigrahi[2], Tapan K. Gandhi[2] ✉

[1]*Centre for Biomedical Engineering, Indian Institute of Technology – Delhi, New Delhi 110 016, India*
[2]*Department of Electrical Engineering, Indian Institute of Technology – Delhi, New Delhi 110 016, India*
[3]*Department of Neurosciences, Fortis Escorts Hospital, New Delhi 110 025, India*
[4]*Neurology and Sleep Centre, New Delhi 110 016, India*
[5]*Department of Neurology, All India Institute of Medical Sciences, New Delhi 110 029, India*
[6]*Department of Neurosurgery, All India Institute of Medical Sciences, New Delhi 110 029, India*
✉ *E-mail: tgandhi@ee.iitd.ac.in*

Published in Healthcare Technology Letters; Received on 13th July 2018; Revised on 15th April 2019; Accepted on 25th April 2019

The significant research effort in the domain of epilepsy has been directed toward the development of an automated seizure detection system. In their usage of the electrophysiological recordings, most of the proposals thus far have followed the conventional practise of employing all frequency bands following signal decomposition as input features for a classifier. Although seemingly powerful, this approach may prove counterproductive since some frequency bins may not carry relevant information about seizure episodes and may, instead, add noise to the classification process thus degrading performance. A key thesis of the work described here is that the selection of frequency subsets may enhance seizure classification rates. Additionally, the authors explore whether a conservative selection of frequency bins can reduce the amount of training data needed for achieving good classification performance. They have found compelling evidence that using spectral components with <25 Hz frequency in scalp electroencephalograms can yield state-of-the-art classification accuracy while reducing training data requirements to just a tenth of those employed by current approaches.

Nomenclature

Symbol	Description
F_s	sampling rate
$D1$	detail coefficients of the first decomposition level
$D2$	detail coefficients of the second decomposition level
$D3$	detail coefficients of the third decomposition level
$D4$	detail coefficients of the fourth decomposition level
$D5$	detail coefficients of the fifth decomposition level
$D6$	detail coefficients of the sixth decomposition level
$A6$	approximation coefficients of the sixth decomposition level
ENE	energy features
SDF	standard deviation features
TP	true positive rate
TN	true negative rate
FP	false positive rate
FN	false negative rate
CA	classification accuracy rate
SN	sensitivity rate
SP	specificity rate
SD	standard deviation across folds
ns	p-value not significant (i.e. >0.05)
*	p-value is significant and ranges between 0.01 and 0.05
**	p-value is significant and ranges between 0.001 and 0.01
***	p-value is significant and lies < 0.001

1. Introduction: Epilepsy is one of the most common neurological disorders which affects more than 65 million individuals worldwide [1]. The hallmark of epilepsy is the enduring propensity of the brain to generate epileptic seizures. According to the International League Against Epilepsy, the epileptic seizures (commonly referred to as 'fits') are transiently occurring recurrent episodes of abnormally excessive and/or synchronous neuronal firings [2]. Its diagnosis is mostly performed using electroencephalography [3]. Neurophysiologist performs the general practise of analysing the recorded electroencephalogram (EEG) to trace the presence of epileptiform patterns and mark its onsets across the time series through visual inspection [1, 4]. However, this process of manual detection is very time-consuming and inefficient especially in the case of long-term EEG recordings [4–6]. Moreover, due to the overlapping symptomatology of epilepsy with other neurological disorders and contamination of EEG signals (especially the extracranial or scalp recordings) with artefacts make the visual scrutinisation procedure very challenging even for an experienced neurophysiologist [4–6]. The repercussions of delayed or misdiagnosis could lead to permanent neurobiological, cognitive, social and psychological impairments [1, 4]. Hence, their need to automate the process of detecting epileptiform patterns in a much more efficient and robust manner have inspired the development of various intelligent models [4–20]. Early attempts [7] have used traditional mimetic techniques that relied on the distinctive attributes of amplitude, slope, height, duration and sharpness values provided by an expert neurophysiologist. Since then, most of the state-of-the-art has adopted a dual scheme, i.e. feature extraction and its classification for the development of automated epileptic seizure detection models [8, 9]. Analysing the frequency bands for epileptic seizure detection has been the foundation for many proposed schemes [5, 10–20]. Still, there has been a lot of disparity in the selection of frequency bands in these studies. While, many researchers have opted to set the decomposition levels up to five [9, 10] and selected all the frequency bands, some of the researchers have even chosen to decompose the same datasets till 11th decomposition levels [12] and selected all the frequency bands. It has already been established that the preferred choice of decomposition levels should be six for feature extraction [18, 19]. However, the problem of selecting the optimum number of frequency bands for efficient seizure detection is still unclear. Some cues could be drawn from the previous research [21] that used bipolar EEG recordings and stated 20–25 Hz as the lower cut-off

for effectively removing electromyogram artefacts through digital filtering. Furthermore, moving in this research direction, notwithstanding findings have been established about using gamma frequencies elicited from intracranial EEG as a marker for epilepsy [22, 23]. Similar scientific questions require further investigations for seizure detection using scalp EEG. Current work attempts to fill this void to achieve accurate seizure detection performance through a selection of an optimum number of frequency bands.

The datasets used in this Letter are described in the next section, and its proceeding section illustrates the proposed methodology. The research outcomes and their corresponding observations are provided in Section 4. Finally, we have summarised the research outcomes and future research directions in the conclusion and future scope section.

2. Datasets: The datasets available from two different repositories are used in this Letter to test the classification of non-seizures versus epileptic seizures. The first datasets are available from a repository created using data recorded from Sir Ganga Ram Hospital (SGRH), New Delhi [5, 18–20, 24]. Its datasets were acquired over 18 epilepsy patients under the supervision of an experienced neurophysiologist using Grass Telefactor Twin3 EEG machine. During data acquisition, the sampling rate was fixed to 400 Hz with a spectral bandwidth of 0.5–70 Hz and a notch filter of 50 Hz. The acquisition was performed using 16 gold-plated surface electrodes placed according to the international 10–20 electrode placement system [25]. After the acquisition, onset and offset points of epileptic seizures were annotated by a trained neuro-technician and cross-checked by an experienced neurophysiologist. On the basis of the annotations, the signals were segmented and saved in two different subsets belonging to non-seizures and epileptic seizures. The subsets of epileptic seizures and non-seizures consisted of 293 and 296 EEG segments, respectively. Here, the duration of each EEG segment was 2.56 s with 1024 samples. To substantiate the research findings, datasets from another repository is formed using recordings of ten epilepsy patients collected at the Neurology and Sleep Centre (NSC), New Delhi [26, 27]. Its datasets were recorded using Comet AS40 EEG machine at a sampling rate of 200 Hz with the same filter settings. The duration of each EEG segment in this repository was 5.12 s with 1024 samples. It consisted of 575 epileptic seizure segments and 529 non-seizure segments. Datasets in both the repositories are available in .MAT format. A sample of an EEG segment taken from each subset available in the NSC repository is shown in Fig. 1.

3. Methodology: The analysis steps implemented in this Letter are as follows, whereas the symbols used in this Letter are listed in the Nomenclature section:

(1) The EEG signals from the first repository are decomposed till the sixth decomposition levels using dual-tree complex wavelet transform (DT-CWT) [28]. The advantage of using this technique is that it is shift invariant in comparison with other commonly used techniques such as discrete wavelet transform (DWT) [14], wavelet packet transform [14] etc. This approach resulted in seven frequency bands (six details and last approximation) which represented the input signal with a frequency range of $0 - F_s/2$ Hz. Here, the sampling rate F_s was equal to 400 Hz for SGRH datasets. The details from first to sixth decomposition levels are represented as $D1$, $D2$, …, $D6$ and the last approximation as $A6$. The range of frequencies for each band is represented by $D1 = 100 - 200$ Hz, $D2 = 50 - 100$ Hz, $D3 = 25 - 50$ Hz, $D4 = 12.50 - 25$ Hz, $D5 = 6.25 - 12.50$ Hz, $D6 = 3.125 - 6.250$ Hz and $A6 = 0 - 3.125$ Hz.

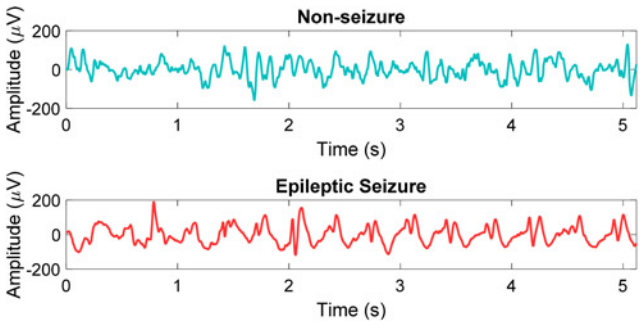

Fig. 1 *Sample of EEG segment taken from each subset available in NSC repository*

(2) Seven sets of datasets are prepared based on the constituent of frequency bands from each category (non-seizure and epileptic seizure). The different constituents of frequency bands kept in these sets of the combination are: (i) $D1$–$D6$ and $A6$; (ii) $D2$–$D6$ and $A6$; (iii) $D3$–$D6$ and $A6$; (iv) $D4$–$D6$ and $A6$; (v) $D5$–$D6$ and $A6$; (vi) $D6$ and $A6$; and (vii) $A6$. As an example, the fourth dataset consists of $D4$, $D5$, $D6$ and $A6$ frequency bands that in terms of total frequency components from 0 to 25 Hz.

(3) It is widely asserted that the neurons require high-energy levels to maintain their normal functioning [29]. The episode of epileptic discharge creates a misbalance in the physiological energy levels. Therefore, energy (ENE) was considered as one of the features for classification and is evaluated using (1). Similarly, the rhythmicity of the brain also gets disturbed during epileptic seizures [1]. Therefore, the measurement of statistical changes from non-seizure condition to epileptic seizure condition also forms an important characteristic [30]. Hence, Standard Deviation feature (SDF) is considered as another feature set and is evaluated using (2)

$$\mathrm{ENE}_i = \sum_{n=1}^{N} |D_{mn}|^2. \tag{1}$$

$$\mathrm{SDF}_i = \sqrt{\left[\frac{1}{N-1}\sum_{n=1}^{N}\left(D_{mn} - \frac{1}{N}\sum_{n=1}^{N} D_{mn}\right)^2\right]}. \tag{2}$$

Here, D_{mn} represents details with $m = 1, 2, \ldots, 6$ (number of decomposition levels) for samples $n = 1, 2, \ldots, N$ (length of the frequency band), $i = 1, 2, \ldots, 7$. The values of ENE_7 and SDF_7 were extracted by replacing D_m with the values of sixth approximation A_6 in (1) and (2), respectively.

(4) The feature sets extracted for each combination of datasets are separately fed into a general regression neural network (GRNN) [31]. This neural network has a feedforward architecture and makes a decision based on probability density function. Therefore, it is relatively fast and suitable for training with even small datasets in comparison with backpropagation networks. The smoothing parameter of the GRNN is set to 0.7.

(5) Cross-validation procedure over ten folds is applied with the train-to-test ratio fixed at 1:9 (i.e. 10% of data used for training and 90% of data used for testing). This step has assured that the robustness of the model is validated against low training.

(6) The performance of the model is assessed by evaluating classification accuracy (CA), sensitivity (SN) and specificity (SP) rates. Additionally, Matthew's correlation coefficient (MCC) which is a balanced statistical measure of an intelligent system corresponding to both SN and SP is also evaluated during each fold. MCC is a unitless measurement given by the equation below:

$$\mathrm{MCC} = \frac{(\mathrm{TP} \times \mathrm{TN}) - (\mathrm{FP} \times \mathrm{FN})}{\sqrt{(\mathrm{TP}+\mathrm{FP})(\mathrm{TP}+\mathrm{FN})(\mathrm{TN}+\mathrm{FP})(\mathrm{TN}+\mathrm{FN})}} \tag{3}$$

where TP is the true positive rate, TN is the true negative rate, FP is the false positive rate and FN is the false negative rate. MCC has recently gained more popularity over other similar measures such

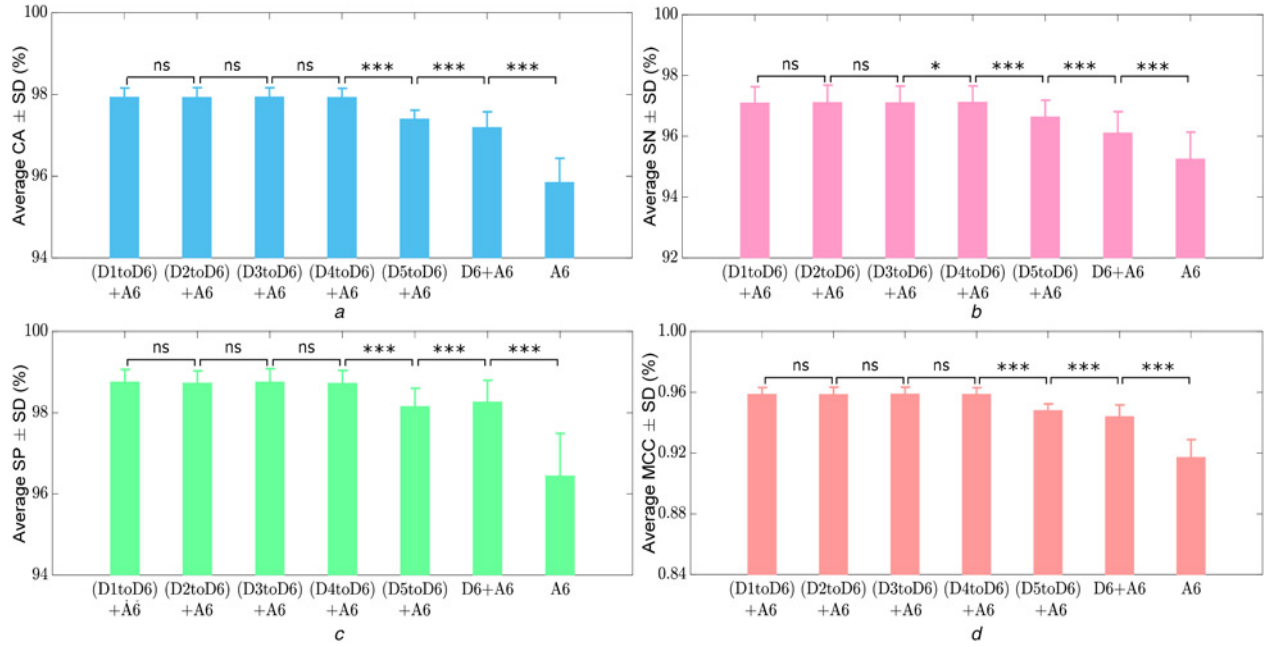

Fig. 2 *Comparison of (a) CA, (b) SN, (c) SP and (d) MCC across different combinations of frequency bands for classification of non-seizures versus epileptic seizures from SGRH datasets using SDF features*
a Comparison of CA
b Comparison of SN
c Comparison of SP
d Comparison of MCC

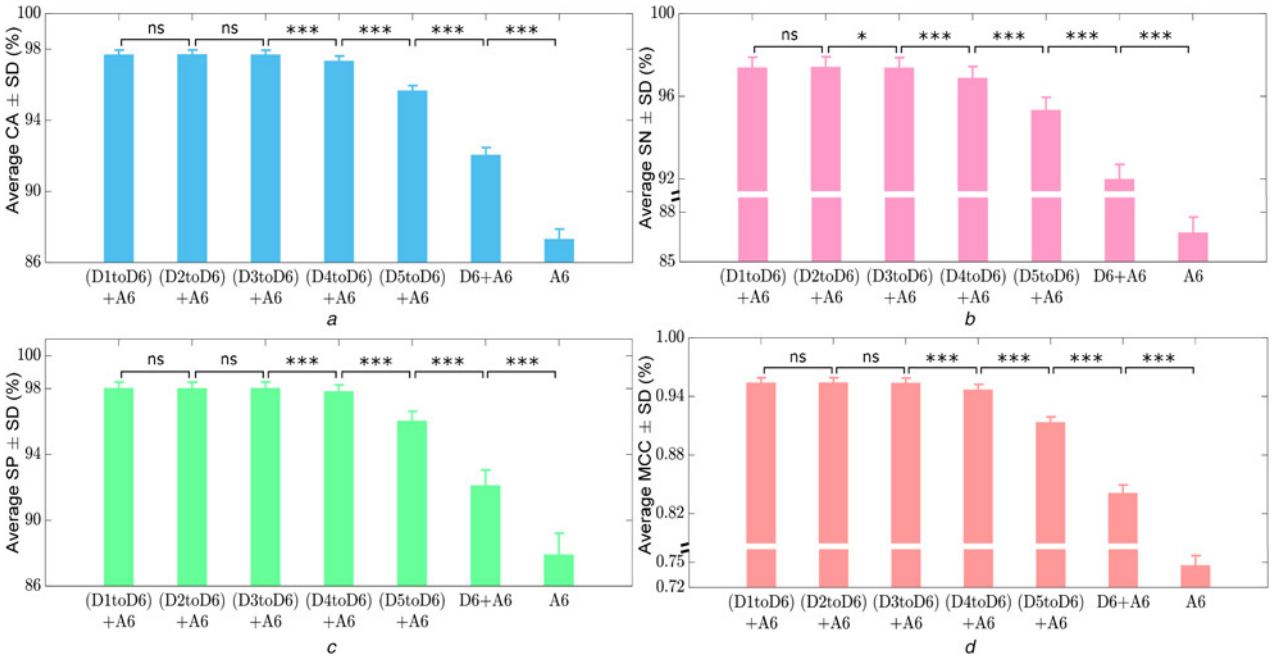

Fig. 3 *Comparison of (a) CA, (b) SN, (c) SP and (d) MCC across different combinations of frequency bands for classification of non-seizures versus epileptic seizures from NSC datasets using SDF features*
a Comparison of CA
b Comparison of SN
c Comparison of SP
d Comparison of MCC

as the area under the curve etc. [32] due to its direct extension to measure more classes and relationship with stability based on its range. The statistical stability of the system could be inferred by the MCC value, which ranges between −1 and 1. The value of MCC close to 1 indicates that all the predicted outcomes are correct; 0 indicates that the predicted outcomes are random guesses; and −1 indicates that all the predicted outcomes are incorrect.

(7) Hypothesis testing is performed by applying Student's *t*-test between the performance parameters evaluated using each feature set of the consecutive combinations of frequency bands. For example, testing the significance level between the performance

doi: 10.1049/htl.2018.5051

measures of all the bands (i.e. $D1$–$D6 + A6$) versus the same performance measure when the only the $D1$ frequency band is ignored (i.e. $D2$–$D6 + A6$). The same procedure is extended to all remaining bands as shown in Fig. 2*a*.

(8) The above steps from 1 to 7 are repeated for the NSC datasets separately. Since the NSC data were collected at a sampling rate of 200 Hz, and hence the range of frequencies for each band in this dataset are $D1 = 50 - 100$ Hz, $D2 = 25 - 50$ Hz, $D3 = 12.50 - 25$ Hz, $D4 = 6.25 - 12.50$ Hz, $D5 = 3.125 - 6.250$ Hz and $D6 = 1.5625 - 3.125$ Hz, $A6 = 0 - 1.5625$ Hz.

4. Results and discussion: The results obtained from the analysis of SGRH datasets using ENE feature sets show that CA equalled 97.936% ± standard deviation (SD) of 0.221% with 95% confidence interval [92.866, 99.733] when all frequency bands, i.e. ($D1$–$D6 + A6$) are considered. There is no significant change in accuracy even without taking into consideration of frequency coefficients from $D1$ to $D3$ frequency bands. However, the CA is dropped significantly ($p < 0.001$) when coefficients from $D4$ frequency band are not considered. This trend is also observed in SN and MCC measures. The CA, SN and MCC with ($D4$–$D6$) + $A6$ frequency band are reported to be 97.934 ± 0.217 [92.864, 99.732], 97.129 ± 0.529 [91.679, 99.418] and 0.959 ± 0.004 [0.899, 0.988]%, respectively. The SP of classification also hold ceiling level performance up to the frequency range ($D4$–$D6$) + $A6$ and degrade statistically ($p < 0.001$) below that frequency band. Considering SDF as another feature, the CA as well as SN and SP follows the similar pattern as shown in Fig. 2.

Table 1 Comparison of the present Letter with few state-of-the-art

Reference	Methodology	Frequency spectrum of features, Hz	Amount of training data, %	Best mean performance reported, %
[11]	dataset(s): University of Bonn (scalp and intracranial EEG) transform(s): DT-CWT feature(s): Fourier features classifier(s): *k*-nearest neighbour	0–86.805	50	CA = 100
[33]	dataset(s): University of Bonn (scalp and intracranial EEG) transform(s): DWT feature(s): singular values calculated from the covariance matrix of two-dimensional (2D) and 3D phase space representations classifier(s): extreme learning machine (ELM), support vector machine (SVM), back propagation neural network, multiplicative-ELM	0.53–85	50	CA ± SD = 98.89 ± 0.32 SN ± SD = 98.92 ± 0.01 SP ± SD = 99.93 ± 0.04
[10]	dataset(s): Royal Brisbane & Women's Hospital (scalp EEG) transform(s): 2D DWT feature(s): flux, flatness, Renyi entropy, mean, variance, skewness, kurtosis, variation coefficient, mean and deviation of instantaneous frequency, complexity, maximum singular values, non-negative matrix factorisation classifier(s): SVM	0–128	99.375	CA = 99.375
[15]	dataset(s): University of Bonn (scalp and intracranial EEG), SGRH (scalp EEG) transform(s): scale invariant feature transformation feature(s): histogram of local binary patterns classifier(s): SVM	0–61.9	>90	CA = 99.45 SN = 99.68 SP = 99.00
[27]	dataset(s): University of Bonn (scalp and intracranial EEG), NSC (scalp EEG) transform(s): discrete cosine transform feature(s): Hurst exponents, autoregressive moving average model parameters classifier(s): SVM	0.1–60	>90	CA = 96.92%
[34]	dataset(s): University of Bonn (scalp and intracranial EEG) transform(s): wavelet packet transform feature(s): fuzzy distribution entropy feature selection using Kruskal–Wallis test classifier(s): *k*-nearest neighbour	0–64	>90	CA ± SD = 99.58 ± 0.19 SN ± SD = 98.89 ± 0.37 SP ± SD = 99.92 ± 0.18
this Letter	dataset(s): SGRH and NSC (both scalp EEG) transform(s): DT-CWT feature(s): ENE, SDF classifier(s): GRNN	0.5–25	10	CA ± SD [CI] = 98.118 ± 0.218[93.146, 99.789] SN ± SD [CI] = 97.489 ± 0.500[92.206, 99.563] SP ± SD[CI] = 98.742 ± 0.305[94.136, 99.929] MCC ± SD[CI] = 0.962 ± 0.004[0.904, 0.990]

In Fig. 2*a*, the CA with $(D4–D6)+A6$ frequency band is significantly higher than CA with $(D3–D6)+A6$ frequency band ($p<0.001$). The similar trend is also observed in SN (Fig. 2*b*), SP (Fig. 2*c*) and MCC (Fig. 2*d*) measures. The above results demonstrate the consideration of frequency range < 25 Hz will hold the best accuracy without compromising in SN and SP. To re-test these findings, the data collected from the NSC repository are also analysed.

The results based on the analysis of NSC datasets using ENE features showed CA=9.388 ± 0.084 [95.224, 99.997]% with $(D3–D6)+A6$ frequency band. The evaluated SN, SP and MCC measures using ENE features within the same frequency range are 98.959 ± 0.156 [94.488, 99.967], 99.855 ± 0.094 [96.091, 100] and 0.988 ± 0.002 [0.942, 0.999]%, respectively. The values of performance parameters using $(D1–D6)+A6$ versus $(D2–D6)+A6$ frequency bands and $(D2–D6)+A6$ versus $(D3–D6)+A6$ frequency bands are not significant, whereas the performance parameters are statistically significant ($p<0.001$) in both $(D3–D6)+A6$ versus $(D4–D6)+A6$ frequency bands and the next adjacent combinations of frequency bands. The results in Fig. 3 show the performance of the model across different combinations of frequency bands considered using SDF features. Apart from its SN rate (Fig. 3*b*) which measured 97.376 ± 0.497 [92.039, 99.520]% with $(D3–D6)+A6$ frequency band and showed significant difference ($p = 0.046$) against $(D2–D6)+A6$ frequency band, all other performance parameters (Figs. 3*a*, *c* and *d*) showed very significant ($p < 0.001$) difference with frequency bands selected within the range of $0 - 25$ Hz. Thus, the results evaluated using SGRH and NSC datasets are in agreement with each other. Also, in line with past findings, the results from the present Letter attest that ENE [20] and SDF [18, 28] are noteworthy features for seizure detection. However, SDF feature sets based classifications (Figs. 2 and 3) are found to be more consistent for both the datasets in our present Letter.

The existing state-of-the-art approaches have reported overall accuracy and statistical performance >97% [11–20]. Therefore, the improvement in classification performance has already reached a saturation point. The contribution from this work with respect to accuracy (98.118 ± 0.218 [93.146, 99.789]%) and statistical performance is still at par with the existing state-of-the-art methods proposed in past (Table 1). However, the listed models have achieved given performance by including frequency spectrum beyond 25 Hz, and the majority of them also used > 50% of data for training their model. Using such a high percentage of datasets for training the model suffers from two main disadvantages. First, it is superficially based on the assumption that the total amount of *annotated* data available is huge which usually is not the case. Second, using such a high percentage of training data from a small sample size of data available could *overtrain* the classifier. Owing to these shortcomings, it becomes highly eminent to test the robustness of the model against low training. In this Letter, only 10% of the data is used for training the classifier. It is also emphasised that many of the past studies [4, 5, 8, 9, 11, 12, 15] have either used intracranial recordings or scalp recordings [6, 13] with all frequency bins available. However, we achieved similar ceiling level performance with limited frequency bins that will reduce the computational cost without compromising the quality of diagnosis.

5. Conclusion and future scope: The experimental data we have presented here demonstrate the importance of frequency components ranging from 0.5 to 25 Hz for the detection of epileptic discharge from scalp recordings. The conventional practise of using a broader range of frequencies is driven in part by the nature of neural signals available intra-cranially. Given that the cranium acts as a strong low-pass filter for electrical field oscillations, it is necessary to adapt analytical techniques to the reduced spectral range available at the scalp. As our results indicate, even with this reduction, a high level of classification performance can be achieved. As a corollary, it needs to be noted that the usage of higher-frequency components in scalp-based recordings can only be expected to worsen classification performance since the high-frequency signals correspond to noise rather than intrinsic neural activity.

The encouraging results we have reported here have allowed us to develop a proof-of-concept epilepsy diagnosis software system for analysing continuous EEG in clinical settings [35]. This is an early demonstration of the clinical relevance of the approach we have presented.

One limitation of this Letter is that unlike the wavelet packet transform, the DT-CWT technique does not provide a very narrow range of frequency bands. Nevertheless, DT-CWT is preferred over its counterparts due to its statistically demonstrable advantage for seizure detection [20]. Further investigations can explore other shift-invariant techniques with a narrower range of frequency bands. Moreover, researchers have long studied the implications of functional connectivity networks and epileptogenic regions [36–38, 39]. Building on the foundation provided by this Letter thus far would lead to better automated detection of epileptiform patterns and thus data confined to epileptiform stages would, in turn, usher better localisation of seizure foci and study its spatiotemporal connections. Future work could also investigate the detection of pre-ictal, ictal, post-ictal and inter-ictal stages. Since each of these stages corresponds to a specific causal factor related to the progression of seizures [40], their investigation would have significant clinical implications.

6. Acknowledgments: The authors thank Mrs. Anu Mol (Senior Neuro-technician at the NSC) for her assistance during the annotation of datasets.

7. Funding and declaration of interests: This work was supported by the Department of Science and Technology (IIT Delhi grant no. RP03060), Government of India.

8 References

[1] Moshé S., Perucca E., Ryvlin P., *ET AL.*: 'Epilepsy: new advances', *Lancet*, 2015, **385**, (9971), pp. 884–898, doi: 10.1016/S0140-6736(14)60456-6

[2] Fisher R.S., Cross J.H., French J.A., *ET AL.*: 'Operational classification of seizure types by the international league against epilepsy: position paper of the ILAE commission for classification and terminology', *Epilepsia*, 2017, **58**, (4), pp. 522–530, doi: 10.1111/epi.13670

[3] Noachtar S., Rémi J.: 'The role of EEG in epilepsy: a critical review', *Epilepsy Behav.*, 2009, **15**, (1), pp. 22–33, doi: 10.1016/j.yebeh.2009.02.035

[4] Duque-muñoz L., Espinosa-oviedo J.J., Castellanos-dominguez C.G.: 'Identification and monitoring of brain activity based on stochastic relevance analysis of short-time EEG rhythms', *Biomed. Eng. Online*, 2014, **13**, (123), pp. 1–20, doi: 10.1186/1475-925X-13-123

[5] Gandhi T.K., Panigrahi B.K., Bhatia M., *ET AL.*: 'Expert model for detection of epileptic activity in EEG signature', *Expert Syst. Appl.*, 2010, **37**, (4), pp. 3513–3520, doi: 10.1016/j.eswa.2009.10.036

[6] Kelly K.M., Shiau D.S., Kern R.T., *ET AL.*: 'Assessment of a scalp EEG-based automated seizure detection system', *Clin. Neurophysiol.*, 2010, **121**, (11), pp. 1832–1843, doi: 10.1016/j.clinph.2010.04.016

[7] Gotman J.: 'Automatic detection of seizures and spikes', *J. Clin. Neurophysiol.*, 1999, **16**, (2), pp. 130–140

[8] Acharya U.R., Sree S.V., Swapna G., *ET AL.*: 'Automated EEG analysis of epilepsy: a review', *Knowl.-Based Syst.*, 2013, **45**, pp. 147–165, doi: 10.1016/j.knosys.2013.02.014

[9] Tzallas A.T., Tsipouras M.G., Dimitrios G., *ET AL.*: 'Automated epileptic seizure detection methods: a review study', in Stevanovic D. (Ed.): 'Epilepsy – histological, electroencephalographic and psychological aspects' (InTech, Rijeka, Croatia, 2012) pp. 1–26, doi: 10.5772/31597

[10] Yusaf M., Nawaz R., Iqbal J.: 'Robust seizure detection in EEG using 2D DWT of time-frequency distributions', *Electron. Lett.*, 2016, **52**, (11), pp. 902–903, doi: 10.1049/el.2016.0630

[11] Chen G.: 'Automatic EEG seizure detection using dual-tree complex wavelet-Fourier features', *Expert Syst. Appl.*, 2014, **41**, (5), pp. 2391–2394, doi: 10.1016/j.eswa.2013.09.037
[12] Xie S., Krishnan S.: 'Wavelet-based sparse functional linear model with applications to EEGs seizure detection and epilepsy diagnosis', *Med. Biol. Eng. Comput.*, 2013, **51**, (1-2), pp. 49–60, doi: 10.1007/s11517-012-0967-8
[13] Chen D., Wan S., Xiang J., *ET AL.*: 'A high-performance seizure detection algorithm based on discrete wavelet transform (DWT) and EEG', *PLoS One*, 2017, **12**, (3), pp. 1–21, doi: 10.1371/journal.pone.0173138
[14] Alickovic E., Kevric J., Subasi A.: 'Performance evaluation of empirical mode decomposition, discrete wavelet transform, and wavelet packed decomposition for automated epileptic seizure detection and prediction', *Biomed. Signal Process. Control*, 2018, **39**, pp. 94–102, doi: 10.1016/j.bspc.2017.07.022
[15] Tiwari A.K., Pachori R.B., Kanhangad V., *ET AL.*: 'Automated diagnosis of epilepsy using key-point-based local binary pattern of EEG signals', *IEEE J. Biomed. Health Inform.*, 2017, **21**, (4), pp. 888–896
[16] Amorim P., Moraes T., Fazanaro D., *ET AL.*: 'Electroencephalogram signal classification based on shearlet and contourlet transforms', *Expert Syst. Appl.*, 2017, **67**, pp. 140–147, doi: 10.1016/j.eswa.2016.09.037
[17] Faust O., Acharya U.R., Adeli H., *ET AL.*: 'Wavelet-based EEG processing for computer-aided seizure detection and epilepsy diagnosis', *Seizure*, 2015, **26**, pp. 56–64, doi: 10.1016/j.seizure.2015.01.012
[18] Gandhi T.K., Panigrahi B.K., Anand S.: 'A comparative study of wavelet families for EEG signal classification', *Neurocomputing*, 2011, **74**, (17), pp. 3051–3057, doi: 10.1016/j.neucom.2011.04.029
[19] Swami P., Gandhi T.K., Panigrahi B.K., *ET AL.*: 'A novel robust diagnostic model to detect seizures in electroencephalography', *Expert Syst. Appl.*, 2016, **56**, pp. 116–130, doi: 10.1016/j.eswa.2016.02.040
[20] Swami P., Gandhi T.K., Panigrahi B.K., *ET AL.*: 'A comparative account of modelling seizure detection system using wavelet techniques', *Syst. Sci., Oper. Log. Modell. Simul. Healthc. Syst.*, 2017, **4**, (1), pp. 41–52, doi: 10.1080/23302674.2015.1116637
[21] Gotman J., Ives J.R., Gloor P.: 'Frequency content of EEG and EMG at seizure onset: possibility of removal of EMG artefact by digital filtering', *Electroencephalographic Clin. Neurophysiol.*, 1981, **52**, (6), pp. 626–639, doi: 10.1016/0013-4694(81)91437-1
[22] Jirsch J.D.: 'High-frequency oscillations during human focal seizures', *Brain*, 2006, **129**, (6), pp. 1593–1608, doi: 10.1093/brain/awl085
[23] Zijlmans M.: 'High-frequency oscillations as a new biomarker in epilepsy', *Ann. Neurol.*, 2012, **71**, (2), pp. 169–178, doi: 10.1002/ana.22548
[24] Gandhi T.K., Chakraborty P., Roy G.G., *ET AL.*: 'Discrete harmony search based expert model for epileptic seizure detection in electroencephalography', *Expert Syst. Appl.*, 2012, **39**, (4), pp. 4055–4062, doi: 10.1016/j.eswa.2011.09.093
[25] Jurcak V., Tsuzuki D., Dan I.: '10/20, 10/10, and 10/5 systems revisited: their validity as relative head-surface-based positioning systems', *Neuroimage*, 2007, **34**, (4), pp. 1600–1611, doi: 10.1016/j.neuroimage.2006.09.024
[26] 'Epilepsy Datasets': Research Gate, 2016. Available at https://www.researchgate.net/publication/308719109_EEG_Epilepsy_Datasets, doi: 10.13140/RG.2.2.14280.32006. Accessed: 30 September 2016, accessed 30 September 2016
[27] Gupta A., Singh P., Karlekar M.: 'A novel signal modeling approach for classification of seizure and seizure-free EEG signals', *IEEE Trans. Neural Syst. Rehabil. Eng.*, 2018, **26**, (5), pp. 925–935, doi: 10.1109/TNSRE.2018.2818123
[28] Selesnick I.W., Baraniuk R.G., Kingsbury N.G.: 'The dual-tree complex wavelet transform', *IEEE Signal Proc. Mag.*, 2005, **22**, (6), pp. 123–151, doi: 10.1109/MSP.2005.1550194
[29] Cloix J.F., Hévor T.: 'Epilepsy, regulation of brain energy metabolism and neurotransmission', *Curr. Med. Chem.*, 2009, **16**, (7), pp. 841–853, doi: 10.2174/092986709787549316
[30] Gajic D., Djurovic Z., Gligorijevic J., *ET AL.*: 'Detection of epileptiform activity in EEG signals based on time-frequency and non-linear analysis', *Front. Comput. Neurosci.*, 2015, **9**, (38), pp. 1–16, doi: 10.3389/fncom.2015.00038
[31] Tomand D., Schober A.: 'A modified general regression neural network (MGRNN) with new, efficient training algorithms as a robust 'black box' tool for data analysis', *Neural Netw.*, 2001, **14**, (8), pp. 1023–1034, doi: 10.1016/S0893-6080(01)00051-X
[32] Jurman G., Riccadonna S., Furlanello C.: 'A comparison of MCC and CEN error measures in multi-class prediction', *PLoS One*, 2012, **7**, (8), pp. 1–8, doi: 10.1371/journal.pone.0041882
[33] Li D., Xie Q., Jin Q., *ET AL.*: 'A sequential method using multiplicative extreme learning machine for epileptic seizure detection', *Neurocomputing*, 2016, **214**, pp. 692–707, doi: 10.1016/j.neucom.2016.06.056
[34] Zhang T., Chen W., Li M.: 'Fuzzy distribution entropy and its application in automated seizure detection technique', *Biomed. Signal Process. Control*, 2018, **39**, pp. 360–377, doi: 10.1016/j.bspc.2017.08.013
[35] Swami P., Panigrahi B.K., Gandhi T.K.: 'A device for automated diagnosis of epilepsy'. Indian Patent field with Application Number 201611043166 on 17 December 2016
[36] Bamidis P.D., Hellstrand E., Lidholm H., *ET AL.*: 'MFT in complex partial epilepsy: spatio-temporal estimates of inter-ictal activity', *Neuroreport*, 1995, **29**, (1), pp. 17–23
[37] Papadelis C., Tamilia E., Stufflebeam S., *ET AL.*: 'High frequency oscillations detected with simultaneous magnetoencephalography and electroencephalography as biomarker of pediatric epilepsy', *J. Vis. Exp.*, 2016, **118**, p. e54883, doi:10.3791/54883
[38] Tamilia E., Madsen J.R., Grant P.E., *ET AL.*: 'Current and emerging potential of magnetoencephalography in the detection and localization of high-frequency oscillations in epilepsy', *Front. Neurol.*, 2017, **8**, (14), pp. 1–18, doi: 10.3389/fneur.2017.00014
[39] Bharath R.D., Panda R., Raj J., *ET AL.*: 'Machine learning identifies 'RSFMRI epilepsy networks' in temporal epilepsy', *Eur. Radiol.*, 2019, **29**, (7), pp. 1–10, doi: 10.1007/s00330-019-5997-2
[40] Fisher R.S., Scharfman H.E., deCurtis M.: 'How can we identify ictal and interictal abnormal activity?', *Adv. Exp. Med. Biol.*, 2014, **813**, pp. 3–23, doi: 10.1007/978-94-017-8914-1_1